VERIFICATION OF OPTIMUM OPERATION METHOD BY SIMULATION FOR THE HVAC SYSTEM WITH A THERMAL STORAGE TANK IN AN ACTUAL BUILDING

Hiromasa Yamaguchi[1*], Harunori Yoshida[2], Naoki Matsushita[3] and Hisataka Kitora[1]

[1] The Kansai Electric Power Co., Inc.

[2] Department of Architecture, Okayama University of Science

[3] Aleph Networks Corporation

Osaka 530-8270, Japan

* yamaguchi.hiromasa@b4.kepco.co.jp, +81-6-7501-0423

ABSTRACT

An optimum operation scheme was applied to the thermal storage system in an actual building and evaluated using measurement data. First, the accuracy of the load prediction was verified. In a trial operation, the expected error percentage (EEP) of the sum of the daily cooling load was 9.8%, which shows the cooling load prediction is sufficiently accurate for practical use. Second, the accuracy of the system simulation of the HVAC system was verified. The simulation error of the total energy consumption was 0.6% on average, and the root mean square error (RMSE) was 4.9 kWh, which indicates that the simulation is sufficiently accurate for estimating the performance of the HVAC system. Finally, the effect of optimum operation was verified by measurement data. The coefficient of performance (COP) of the heat source system was improved by 3.5% and the COP of the entire system was improved by approximately 10.9% with optimum operation.

INTRODUCTION

The thermal storage system in a building's HVAC system theoretically exemplifies the technological advances of energy conservation as well as reduction of CO_2 emissions. It has been reported, however, that energy conservation is not achieved in actual operation due to non-optimal system operation. To solve this problem, for example, investigation of operational procedures which intend to minimize energy consumption in a stratified chilled water heat storage tank was reported using measured data of a real system (Bahnfleth, W.P. et al. 1994.) or a method to optimize the set points of HVAC system was discussed (Lu Lu et al. 2005.). However, simulation has not been applied to obtain a total optimal operation strategy of an air-conditioning system with a thermal storage tank. A part of the authors previously proposed a basic methodology for optimum operation of a thermal storage water system based on simulation technology and thermal load prediction (Yoshida et al., 1997). Also, the effect of optimum operation by simulation (Yoshida et al., 1999, 2001, Yamaguchi et al., 2005) was shown in simulation basis. In the present paper, the optimum operation scheme is applied to the heat source system with a thermal storage tank in an actual building and validated using measured real data.

PROFILE OF THE BUILDING

The building in which the optimum operation was applied is shown in Figure 1. It is an office building built in 1999 in Fukui Prefecture, which is located in the central northern part of Japan. The building has five stories above ground and one below. The total floor area is 10,724 m^2. This building has two HVAC systems. One is a system with a thermal storage tank for the offices and the other is a system without a thermal storage tank for the machine rooms. The optimum operation scheme was applied to the system for the offices. Figure 2 shows the diagram of the HVAC system for the offices. It includes one air source heat pump and one reciprocating chiller. The air-conditioning system is an all-air, single-duct system which can supply a variable air volume.

Figure 1 Appearance of the building
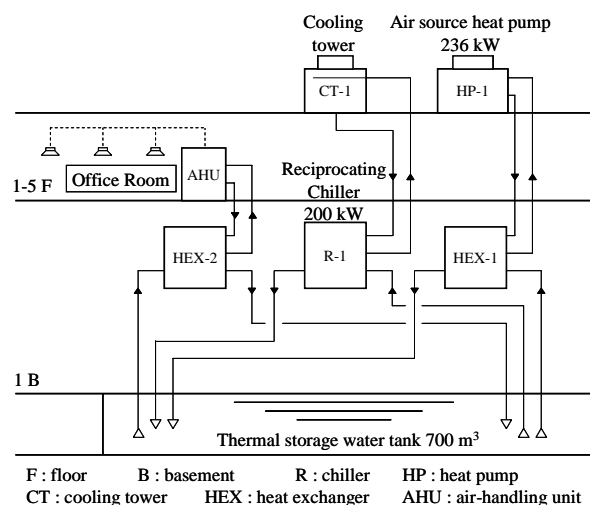
Figure 2 HVAC system diagram of the office

OPTIMUM OPERATION ALGORITHM

The optimum operation algorithm for the HVAC system with a thermal storage tank consists of four blocks: prediction of cooling load, determination of required heat storage, system simulation, and optimum system operation control. Each block is discussed separately in the following sections.

The algorithm block to predict cooling load

The first algorithm block predicts the cooling load for the next day. The prediction method is based on a previous report (Yoshida et al., 1997), although two improvements were added. One improvement is correction of the cooling load by the running ratio of the air-handling units (AHUs). The original method assumed that all AHUs operate on the same schedule, even though buildings, including the test building, have many AHUs with different operating schedules. The other improvement is the prediction of the outside air humidity ratio. The original method used information from weather forecasts. But measurement data in the recent past was used for the building in the current study because the weather forecasts did not correctly predict the outside air humidity ratio.

The algorithm block to determine required thermal storage

The second block determines the required thermal storage on the basis of the predicted cooling load. The required thermal storage for the next day is defined as follows.

$$q_d = q_a + q_p + q_l + q_r \qquad (1)$$

where,

q_d : required thermal storage [kJ]

q_a : predicted building load [kJ]

q_p : generated heat by circulation pumps for chilled water [kJ]

q_l : heat loss through storage tank walls [kJ]

q_r : heat to recover average temperature of the tank to standard [kJ]

The algorithm block to simulate the HVAC system

In the third block, equipment models expressed as numerical expressions were used to construct the HVAC system model. Total energy consumption of the HVAC system on the next day was simulated using this model.

The algorithm block to control optimum system operation

The last block determines how to control the system in an optimum manner. Variables for optimum operation are the setpoint temperature of the chiller, θ_{set}, and chiller operating time at night, t_{ope}. The combination of θ_{set} and t_{ope} to minimize the total system energy consumption is determined based on the flow chart shown in Figure 3. Constraints are the water flow rate of the secondary pump, which

supplies chilled water to the cooling coil, and the operating time of the chiller.

The constraints in optimization are as follows:

$$\dot{m}_{ac} \leq \dot{m}_{ac,d} \; , \; t_{ope} \leq 10$$

where,

$\dot{m}_{ac}$: water flow rate of the secondary pump [kg/s]

$\dot{m}_{ac,d}$: rated value of $\dot{m}_{ac}$ [kg/s]

The operating schedule of the chiller at night should be shifted to the morning because the heat loss from the tank is decreased and the outside air temperature is lower. Therefore, in optimum operation, the chiller is started t_{ope} before 7:00 (24-hour clock), which is one hour before the air-conditioning start-up. This operation is designated "early morning operation."

The calculation procedure in this block is as follows.

1. θ_{set} is set to the default value (13°C).

2. Chiller operating time t_{ope}, which is necessary to generate the required thermal storage, is calculated as follows. The chiller is started at 22:00, when the "night-time tariff" of electricity is applied. When the required thermal storage is generated, the chiller is stopped. The time taken to generate required thermal storage is adopted as t_{ope}.

3. Early morning operation is simulated using t_{ope} and the total energy consumption of the system is estimated.

4. θ_{set} is increased by 0.1°C from 13 to 20°C, and steps 2 and 3 are repeated about all combinations of θ_{set} and t_{ope}. As a result, optimum solutions of θ_{set} and t_{ope} are found, which minimizes the total energy consumption of the system.
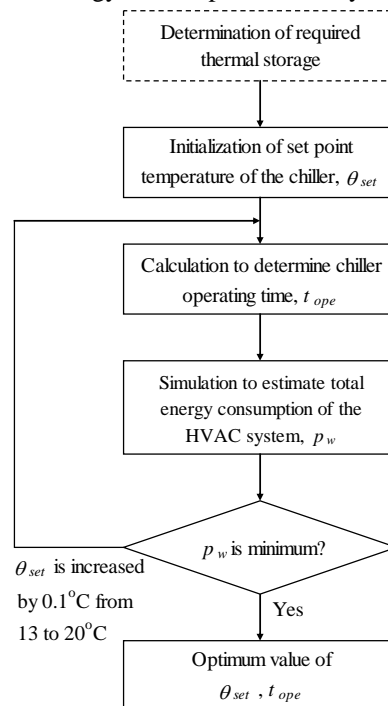
Figure 3 Flow chart of optimum operation

To obtain true optimum operation the set of θ_{set} for each time step throughout a sequence of storage operation is required. But in the present operation a constant θ_{set} is used because of simplicity. Therefore the operation should be called suboptimal not fully optimum. The system has two heat sources. Both heat sources use the same value for t_{ope} to reduce computation time. Although t_{ope} and θ_{set} may actually be the same, a difference of 1°C is given between the two heat sources in consideration of the heat exchange loss. The computation time to find the optimum solution is approximately 15 minutes.

ACCURACY OF LOAD PREDICTION

The cooling load prediction based on the original method (Yoshida et al., 1997) and the two improvements were applied to the building and a trial run commenced in 2007. The running ratio of AHUs was calculated based on the operating schedule of each AHU, which is input by the operator beforehand. The prediction results from June to August are shown in Figures 4 to 6. On five days (6/2, 6/30, 7/1, 7/7, 7/8), the predicted cooling load was zero because the operator did not input the operating schedules of the AHUs beforehand due to a holiday. The result of the trial run except for these five days showed that the expected error percentage (EEP) of the daily summed cooling load was 9.8% and the EEP of the hourly summed cooling load was 12.7%. EEP is the percentage of RMSE to the maximum load. Because the operating schedules of AHUs change to adapt to the daily building use, the actual ratio of AHUs was different from that used for the prediction. Thus, an incorrect schedule can decrease the predicting accuracy.
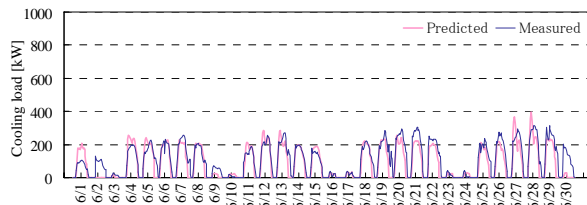
Figure 4 Result of cooling load prediction (June)
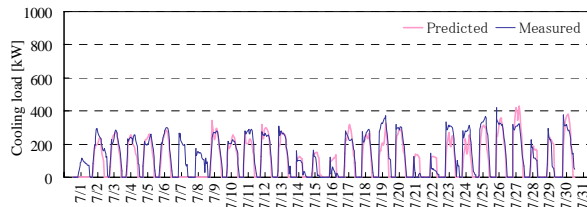
Figure 5 Result of cooling load prediction (July)
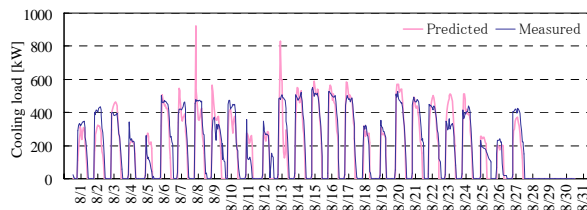
Figure 6 Result of cooling load prediction (August)

MODELING OF HVAC SYSTEM

A diagram of the HVAC system in the building is shown in Figure 7. Each equipment model is developed as numerical expressions. These models are then connected to compose the whole HVAC system.
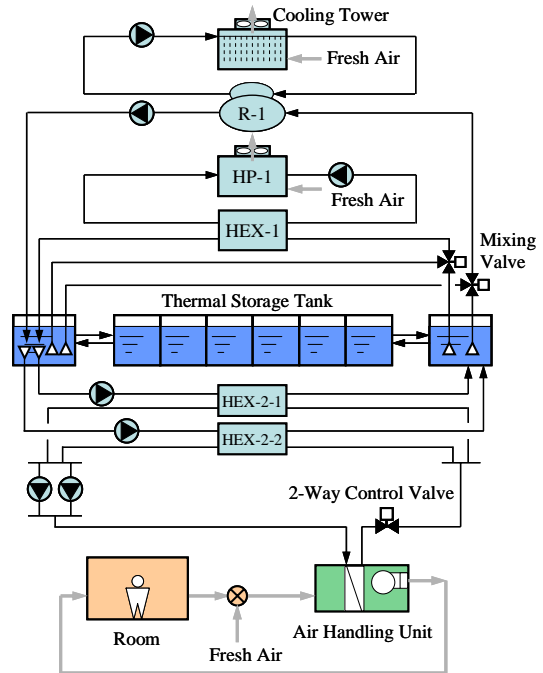
Figure 7 System diagram of the HVAC system

Modeling of HVAC equipment

The HVAC equipment modeling process is as follows. 1) Each model is developed using the performance curve obtained from manufacturers. 2) The developed model is refined by a calibration coefficient, which minimizes the difference between the measured data and simulated data.

The equipment models developed were the reciprocating chiller (R-1), air source heat pump (HP-1), cooling tower (CT), heat exchanger (HEX), air mixing chamber (MC), fan (F), secondary chilled water pump (variable water volume) (PC-V), three-way mixing valve (MV), and cooling coil (CC). For the cooling water pump and primary chilled water pump (constant water volume), power consumption is almost constant. So the value of the short-term measurement of the power consumption (about 1 minute) is used as the estimating value. The models of R-1, HP-1, HEX, MC and F are characterized in the following equations. Other equipment models (PC-V, MV and CC) were based on the previous report (Yamaguchi et al., 2005).

1) Reciprocating chiller (R-1)

The reciprocating chiller model is shown in Equations (2) to (6).

$$Q_{er} = \left(a_1\theta_{eir}^2 + a_2\theta_{eir} + a_3\right) \cdot \left(a_4\theta_{ci}^2 + a_5\theta_{ci} + a_6\right) + a_7 \quad (2)$$

$$E_r = \left(b_1\theta_{eir}^2 + b_2\theta_{eir} + b_3\right) \cdot \left(b_4\theta_{ci}^2 + b_5\theta_{ci} + b_6\right) + b_7 \quad (3)$$

$$Q_c = Q_{er} + E_r \quad (4)$$

$$\theta_{eor} = \theta_{eir} + Q_{er}/(c_p \dot{m}_{re}) \qquad (5)$$

$$\theta_{co} = \theta_{ci} + Q_c/(c_p \dot{m}_c) \qquad (6)$$

where,

Q_{er} : actual load [kW]

Q_c : heat rejection at condenser [kW]

E_r : power consumption [kW]

θ_{eir} : inlet temperature of chilled water [^{o}C]

θ_{ci} : inlet temperature of cooling water [^{o}C]

θ_{eor} : outlet temperature of chilled water [^{o}C]

θ_{co} : outlet temperature of cooling water [^{o}C]

$\dot{m}_{re}$: flow rate of chilled water [kg/s]

$\dot{m}_c$: flow rate of cooling water [kg/s]

c_p : specific heat of water [kJ/kgK]

$a_1 - a_7$: coefficients for actual load

$b_1 - b_7$: coefficients for power consumption

Calibrated power consumption is determined by Equation (7).

$$E'_r = k_r \cdot E_r \qquad (7)$$

where,

E'_r : calibrated power consumption [kW]

k_r : calibration coefficient

2) Air source heat pump (HP-1)

The air source heat pump model is shown in Equations (8) to (10).

$$Q_{eh} = \left(c_1\theta_{eih}^2 + c_2\theta_{eih} + c_3\right)\cdot\left(c_4\theta_{oa}^2 + c_5\theta_{oa} + c_6\right) + c_7 \qquad (8)$$

$$E_h = \left(d_1\theta_{eih}^2 + d_2\theta_{eih} + d_3\right)\cdot\left(d_4\theta_{oa}^2 + d_5\theta_{oa} + d_{oa}\right) + d_7 \qquad (9)$$

$$\theta_{eoh} = \theta_{eih} + Q_{eh}/(c_p \dot{m}_{he}) \qquad (10)$$

where,

Q_{eh} : actual load [kW]

E_h : power consumption [kW]

θ_{eih} : inlet temperature of chilled water [^{o}C]

θ_{eoh} : outlet temperature of chilled water [^{o}C]

θ_{oa} : outside air temperature [^{o}C]

$\dot{m}_{he}$: flow rate of chilled water [kg/s]

$c_1 - c_7$: coefficients for actual load

$d_1 - d_7$: coefficients for power consumption

HP-1 has two compressors and the actual load is controlled for four stages (25%, 50%, 75%, 100%) according to the inlet temperature of the chilled water. When the output is controlled to 75% or less (partial load), the actual load and the power consumption are calculated by multiplying Q_{eh}, E_h by partial load coefficients r_q, r_e, respectively. The power consumption is calibrated by Equation (11).

$$E'_h = k_h \cdot E_h \qquad (11)$$

where,

E'_h : calibrated power consumption [kW]

k_h : calibration coefficient

3) Heat exchanger

The heat exchanger model is shown in Equations (12) to (18). The primary side outlet water temperature $\theta_{1,o}$ and secondary side outlet water temperature $\theta_{2,o}$ are calculated by solving simultaneous equations, whose unknown variables are $\theta_{1,o}$ and exchanged heat Q.

$$Q = U_d A T_{md} \qquad (12)$$

$$T_{md} = \left(\Delta T_1 - \Delta T_2\right)/\ln\left(\Delta T_1/\Delta T_2\right) \qquad (13)$$

$$\Delta T_1 = \theta_{2,i} - \theta_{1,o}, \ \Delta T_2 = \theta_{2,o} - \theta_{1,i}$$

$$\theta_{2,o} = \theta_{1,i} + \Delta\theta \qquad (14)$$

$$U_d = 1/U_{c1} + 1/R_d + 1/U_{c2} \qquad (15)$$

$$U_{c1} = \left(\dot{m}_1/\dot{m}_{1,d}\right)^{0.8} U_{c1,d}, U_{c2} = \left(\dot{m}_2/\dot{m}_{2,d}\right)^{0.8} U_{c2,d} \qquad (16)$$

$$Q_1 = c_p\dot{m}_1\left(\theta_{1,o} - \theta_{1,i}\right), Q_2 = c_p\dot{m}_2\left(\theta_{2,i} - \theta_{2,o}\right) \qquad (17)$$

$$Q = Q_1 = Q_2 \qquad (18)$$

where,

Q : exchanged heat [kW]

U_d : overall heat transfer coefficient [kW/(m^{2}K)]

U_c : heat transfer coefficient [kW/(m^{2}K)]

$U_{c,d}$: rated value of U_c [kW/(m^{2}K)]

R_d : coil-fouling factor [kW/(m^{2}K)]

A : heat transfer surface area [m^2]

T_{md} : log mean temperature difference [K]

θ : water temperature [^{o}C]

$\Delta\theta$: differential between $\theta_{2,o}$ and $\theta_{1,i}$ [K]

$\dot{m}$: water flow rate [kg/s]

$\dot{m}_{2,d}$: rated value of $\dot{m}$ [kg/s]

1 : high temperature side

2 : low temperature side

in : inlet

out : outlet

The coil-fouling factor is calibrated by Equation (19).

$$R' = k \cdot R_d \qquad (19)$$

where,

R' : calibrated coil-fouling factor [kW/(m^{2}K)]

k : calibration coefficient

4) Air mixing chamber

The temperature and humidity ratios of mixing air are calculated using the outside air temperature, outside air humidity ratio, outside air flow rate, and return air flow rate, as shown in Equations (20) and (21).

$$\theta_m = \left(\dot{m}_{oa} \cdot \theta_{oa} + \dot{m}_{ra} \cdot \theta_{ra}\right)/\left(\dot{m}_{oa} + \dot{m}_{ra}\right) \qquad (20)$$

$$x_m = \left(\dot{m}_{oa} \cdot x_{oa} + \dot{m}_{ra} \cdot x_{ra}\right)/\left(\dot{m}_{oa} + \dot{m}_{ra}\right) \qquad (21)$$

where,

$\dot{m}_{oa}$: outside air flow rate [kg/s]

$\dot{m}_{ra}$: return air flow rate [kg/s]

x_m : mixing air humidity ratio [kg/kgDA]

x_{oa} : outside air humidity ratio [kg/kgDA]

x_{ra} : return air humidity ratio [kg/kgDA]

θ_m : mixing air temperature [°C]

θ_{ra} : return air temperature [°C]

5) Fan

Power consumption of the fan is calculated using the air flow rate, shown in Equation 22. Coefficients of Equation (22) are obtained by the short-term measurement data of the power consumption and the frequency.

$$E_f = a_f\left(\dot{m}_a / \dot{m}_{a,d}\right) + b_f \qquad (22)$$

where,

$\dot{m}_a$: air flow rate [kg/s]

$\dot{m}_{a,d}$: rated value of $\dot{m}_a$ [kg/s]

E_f : power consumption of fan [kW]

a_f , b_f : coefficients

Accuracy of equipment model

The calculated values of the actual load and the power consumption of R-1 and HP-1 are shown in Figures 8 to 13 and compared with the measured values. The accuracy of both models improved greatly as a result of calibration.
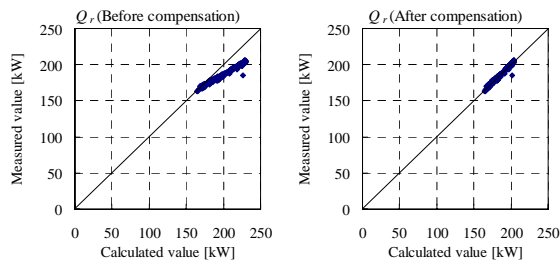
Figure 8 Accuracy of actual load of R-1 (Q_r) before and after calibration
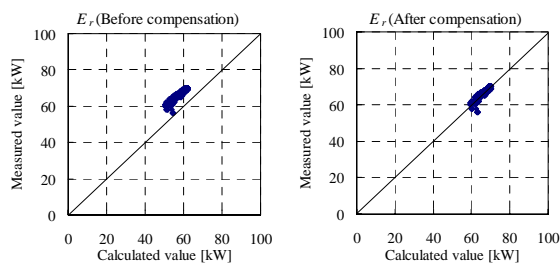
Figure 9 Accuracy of power consumption of R-1 (E_r) before and after calibration
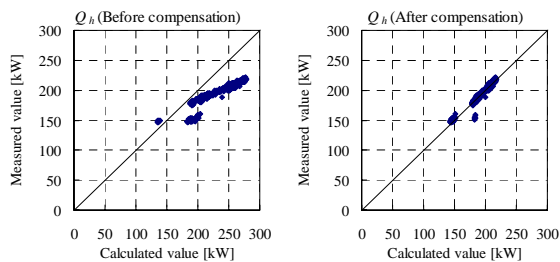
Figure 10 Accuracy of actual load of HP-1 (Q_h) before and after calibration
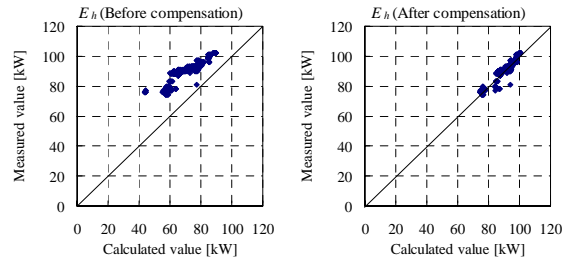
Figure 11 Accuracy of power consumption of HP-1 (E_h) before and after calibration
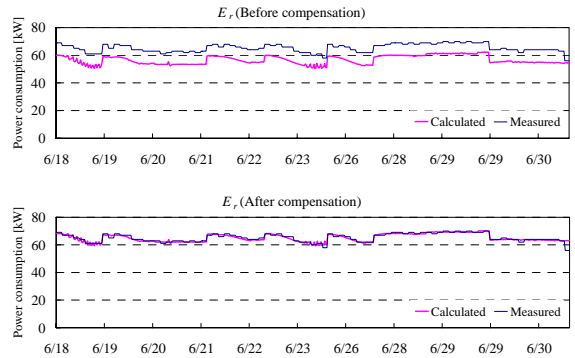
Figure 12 power consumption of R-1 (E_r) before and after calibration
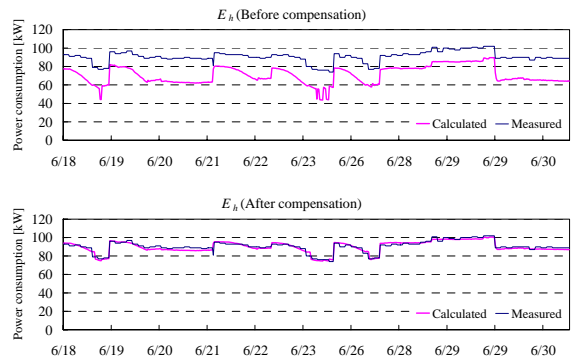
Figure 13 power consumption of HP-1 (E_h) before & after calibration

Modeling of HVAC system

To construct the entire HVAC system, the calibrated equipment models are connected as shown in Figure 7.

Accuracy of HVAC system model

Calculated total power consumption was compared with the measured value in the condition that the heat source operating schedules are fit to the actual operation to validate system model accuracy. The calculation period was 8/20 to 8/23. The simulation error of the total energy consumption excluding the load prediction error was 0.6% on average and the RMSE was 4.9 kWh, which indicates that the simulation is sufficiently accurate for estimating the performance of the HVAC system. The high accuracy is obtained due to the contribution of the model calibration. The error seen at the start time of the heat source causes the inaccurate calculation of the capacity control of HP-1.
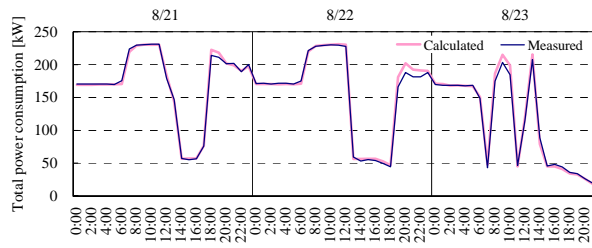
Figure 14 Accuracy of total power consumption

VERIFICATION OF OPTIMUM OPERATION BY EXPERIMENT

Method to verify optimum operation by experiment

The optimum and non-optimum operation were alternately selected, and the results were compared. Non-optimum means the traditional operation that the thermal storage tank are full every night. Carrying out the optimum mode and the non-optimum mode operation alternately as shown in Table-1.

Table 1 Alternating schedule of the operation mode

Name	Operation mode	Times	Period
O-1	Optimum	1st	7/23 to 7/29
N-1	Non-optimum	1st	7/31 to 8/6
N-2	Non-optimum	2nd	8/10 to 8/16
O-2	Optimum	2nd	8/17 to 8/23
O-3	Optimum	3rd	8/24 to 8/30
O-4	Optimum	4th	8/31 to 9/6
N-3	Non-optimum	3rd	9/7 to 9/13
O-5	Optimum	5th	9/15 to 9/20
N-4	Non-optimum	4th	9/21 to 9/27
O-6	Optimum	6th	9/29 to 10/4
N-5	Non-optimum	5th	10/6 to 10/11

Non-optimum operation

In non-optimum operation, θ_{set} is set to a constant 13°C. The target rate of the stored thermal energy is set to 100% at 8:00 and 40% at 22:00 hrs. In daytime operation, if the rate of the stored thermal energy is α % lower than the target line, the heat sources are re-started. Here, α can be set for each time zone. The target rate of the stored thermal energy at 22:00 is set to 40% because the capacity of the thermal storage tank is larger than the heat generated by the heat sources for ten hours. If the target rate of the stored thermal energy at 22:00 is set to 0%, thermal storage at 8:00 does not approach 100%.
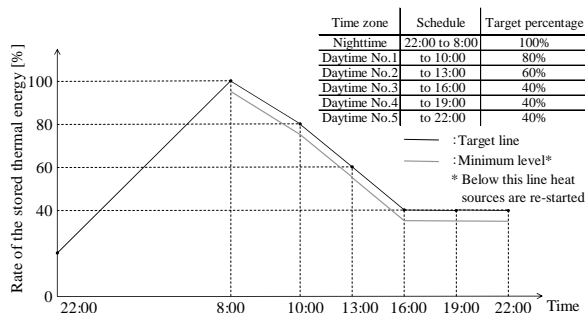
Figure 15 Control of non-optimum operation

Comparison of operation results

1) Setpoint temperature of heat source

Inlet water temperatures of R-1 and HEX-1 are shown in Figure 16. The actual measured values are almost 13°C in the non-optimum operation period when the setpoint was 13°C. In contrast, values are higher than 13°C in the optimum operation period. This confirms the effect of optimization.
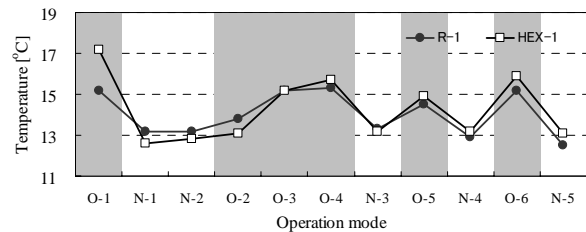
Figure 16 Inlet water temperature of R-1 and HEX-1

2) COP of heat source and heat source system

The improvement ratios of average COP of R-1, HP-1, and the heat source system are shown in Figure 17. The improvement ratio is a value in which COP of a period is divided by COP of the M-2 period, when COP is the lowest. On average in all periods, heat source system COP of the optimum operation exceeded the non-optimum operation by approximately 3.5%, although the influence of the outside air temperature, etc., was contained. The correlation between the inlet chilled water temperature and the actual load (or the power consumption) is shown in Figure 18. Both the actual load and the power consumption increase when the inlet chilled water temperature rises. Because the increasing rate of the actual load is larger than that of the power consumption, heat source COP improves. However, the effect is small for R-1. R-1 is an old type of reciprocating chiller and the refrigerative pressure control is not precise. A greater effect can be expected with the latest equipment, such as a centrifugal chiller or screw chiller.
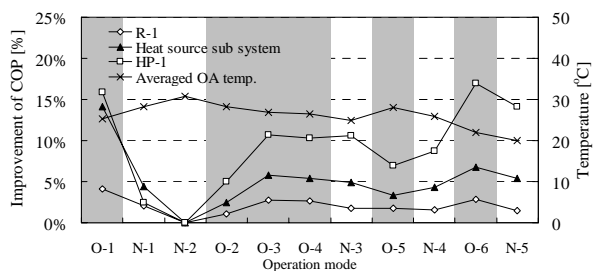
Figure 17 Improvement ratio of heat source COP

3) System COP

The improvement ratio of the system COP is shown in Figure 19 and the average temperature in the tank is shown in Figure 20. On average in all periods, the system COP of the optimum operation exceeded the non-optimum operation by approximately 10.9%. Heat-source COP improved as a result of raising the inlet temperature and schedule shift to the morning.

R-1

HP-1
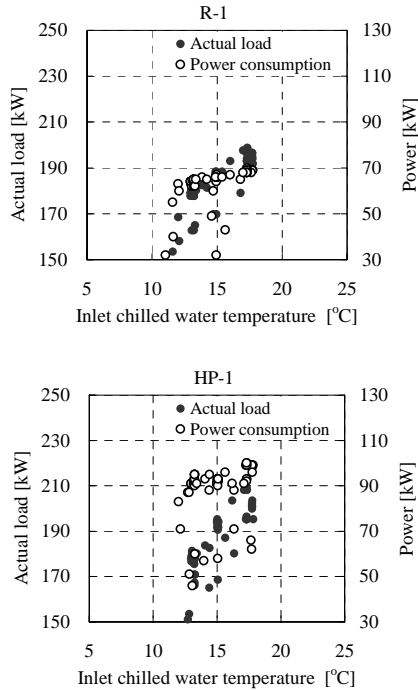
Figure 18 Correlation between the inlet chilled water temperature and actual load (or power consumption)

The heat loss from the tank decreased as a result of keeping the required minimum thermal storage. These are the causes of the improved system COP. Moreover, as a result of heat source COP improvement, the heat source operating time is shortened. The power consumption of the pumps is also reduced. However, a large effect does not appear in all periods. Especially, the difference of system COP is small for the period when the outside air temperature is high. Conversely, system COP of optimum operation exceeds that of the non-optimum operation when the outside air temperature is low. The optimum operation becomes effective in the period when the required heat is small because θ_{set} can be set higher. In contrast, the effect of the optimum operation is small when the peak load occurs because θ_{set} is similar to that of the non-optimum operation.
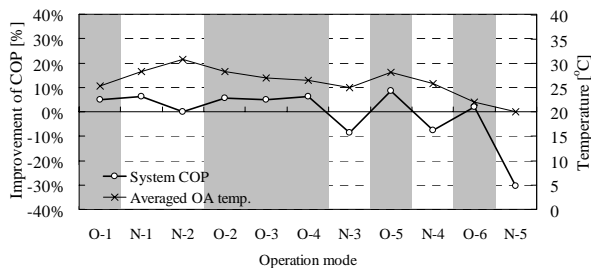
Figure 19 Improvement ratio of system COP
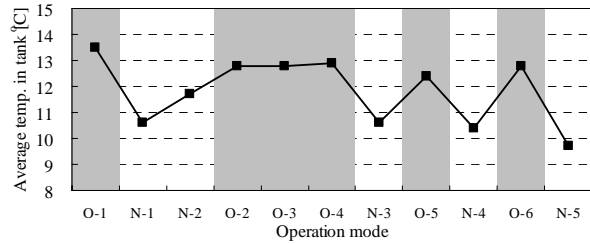
Figure 20 Average temperature in the tank

VERIFICATION OF OPTIMUM OPERATION BY SIMULATION

Methods to verify optimum operation by simulation

In the previous chapter the effect of the optimum operation was estimated by carrying out the optimum operation and the non-optimum operation alternately and comparing these. However, because it is based on the comparison of the operations carried out in the periods when the temperature and cooling load are different, this method doesn't show the effect of the optimum operation strictly. It is desirable to compare the optimum operation with non-optimum operation in the same conditions to verify the effect of the optimum operation more accurately. This comparison is possible by simulation. So the following two types of simulation were performed.

1) Simulation-A1: The simulation assumes the optimum operation is performed for the period when the non-optimum operation is in effect (N1-N5).

2) Simulation-A2: The simulation assumes the non-optimum operation is performed for the period when optimum operation is in effect (O1-O6).

Simulation result and consideration

The system COP of the heat source system by simulation is shown in Figures 21 and 22 for simulation methods A1 and A2, respectively. The heat source system COP improves by 6% to 10% if optimum operation is performed in the non-optimum operation period, as shown in Figure 21. In contrast, the heat source system COP decreases by approximately 3% or less if non-optimum operation is performed in the optimum operation period (Figure 22).
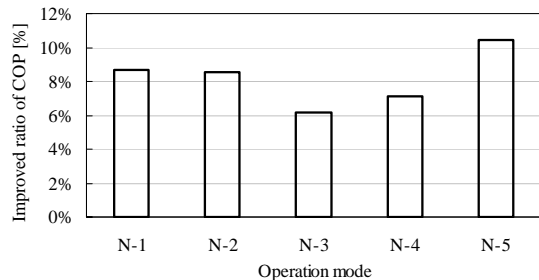
Figure 21 Heat source system COP by simulation-A1
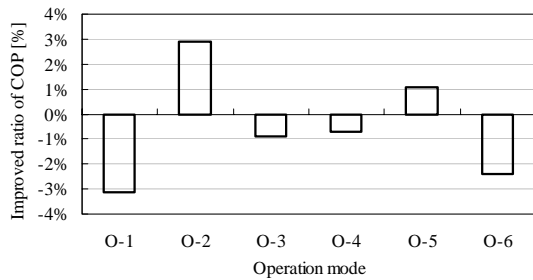
Figure 22 Heat source system COP by simulation-A2

System COP by simulation is shown in Figures 23 and 24. The system COP improves from 0% to 37% if optimum operation is performed during the non-optimum operation period, as shown in Figure 23. In contrast, the system COP decreases by 2% to 8% if the non-optimum operation is performed in the optimum operation period (Figure 24). The effect of optimum operation was simulated accurately. In future work, simulations will be performed to show the effect of optimum operation when the heat source is changed.
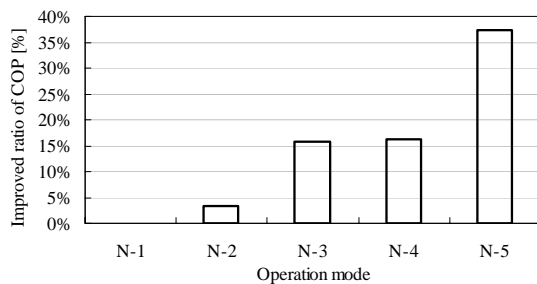
Figure 23 System COP by simulation-A1
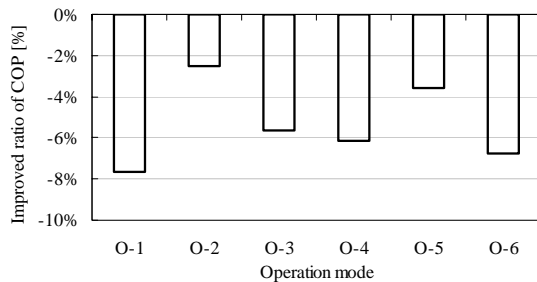
Figure 24 System COP by simulation-A2

CONCLUSION

In this report, the optimum operation of the HVAC system with a thermal storage water tank, based on simulation technology and thermal load prediction, was applied to an actual building. The effect was shown by measurement and simulation. The conclusions are presented as follows.

1. It was confirmed that the cooling load prediction is accurate enough for practical use. The EEP of the daily summed cooling load was 9.8% and the EEP of the hourly summed cooling load was 12.7%.

2. The accuracy of system simulation of the HVAC system was verified. The simulation error of the total energy consumption excluding the load prediction error and control strategy variation error was 0.6% on average and the RMSE was 4.9 kWh, which indicates that the simulation is sufficiently accurate for estimating the performance of the HVAC system. It must be pointed out that the calibration of each equipment model is indispensable to obtain the high accuracy.

3. The effect of optimum operation was verified by measurement and simulation. The heat source system COP improved by 3.5% and the system COP improved by approximately 10.9% by optimum operation based on the measured value. In the simulation, the heat source system COP improved by 3.9% and the system COP improved by approximately 8.0%.

As a result of the present study, the optimum operation of HVAC system with a thermal storage water tank based on simulation technology and thermal load prediction was confirmed to work effectively in an actual building.

REFERENCES

Bahnfleth, W.P. Joyce, W.S. 1994. Energy use in a district cooling system with stratified chilled-water storage, ASHRAE Transactions Vol.100(1), pp.1767-1778

Yamaguchi.H., Yoshida.H. 2005. Develop-ment of Optimal Operation Schemes for HVAC Systems with a Thermal Storage Tank and Verification in Simulation Bases using Real Building Data, Transactions of SHASE, No. 105, pp.1-11

Yoshida.H., Inooka.T. 1997. Rational Operation of A Thermal Storage Tank with Load Prediction Scheme by ARX Model Approach, Proceeding of Building Simulation '97 Prague, Czech Republic, pp. 79-86

Yoshida.H., Goto.Y. 1999. Development of Optimal Operation of Thermal Storage Tank and the Validation by Simulation Tool, Proceeding of Building Simulation '99 Kyoto, Japan, BS99-088

Yoshida.H., Yamaguchi.H. 2001. Optimal Operation of a HVAC System with a Thermal Storage Water Tand, Proceeding of Building Simulation '01 Rio de Janeiro, Brazil, pp.1249-1256

Lu Lu, Wenjian Cai, Lihua Xie, Shujiang Li, Yeng Chai Soh 2005. HVAC system optimization – in building section, Energy and Buildings, Vol.37, pp.11-22